

Variations of the Northern Hemisphere Atmospheric Energetics: 1948–2000*

QI HU, Y. TAWAYE, AND S. FENG

Climate and Bio-Atmospheric Sciences Group, School of Natural Resource Sciences, University of Nebraska at Lincoln, Lincoln, Nebraska

(Manuscript received 16 January 2003, in final form 12 June 2003)

ABSTRACT

Many studies have shown evidence of a major climate change in the late 1970s and early 1980s. The change comprises a reversal of the sea surface temperature anomaly pattern in the North Pacific Ocean, a lowering of the atmospheric geopotential height in the North Pacific, altered frequency and intensity of cyclones/anticyclones and severe storms in the mid- and high latitudes, along with an “abrupt” increase of the Northern Hemisphere (NH) average surface air temperature. What do these changes mean in terms of the nature of the NH atmospheric circulation in the warmer climate? Do they indicate changes of the atmospheric energy cycle and conversion/exchange between various energy forms in the atmosphere? In which latitude regions are such changes in the energetics most significant? These are some of the questions examined in this study for the period 1948–2000 using the NCEP–NCAR reanalysis data. Major results of this study show significant increases of both the NH mean and eddy kinetic energy in boreal summer and winter in the recent two decades since 1980. The NH mean available potential energy has remained unchanged, however, even though the generation of the available potential energy has increased after 1980. The extra available potential energy generated is found to be converted to the kinetic energy by a more efficient conversion from the available potential energy to the kinetic energy in the warmer climate. The increase of the NH kinetic energy is attributed to an increase of the midlatitude kinetic energy because the kinetic energy in the tropical region has decreased slightly after 1980. Additional analysis of the NH energetics in wavenumber domain further reveals an increase of the kinetic energy for motions of planetary to regional scales. Increases of both the mean and eddy kinetic energy in the mid- and high latitudes is consistent with the reports of rising intensity of synoptic systems, cyclones and anticyclones, and severe storms in the recent two decades.

1. Introduction

In the late 1980s, Nitta and Yamada (1989) identified a large increase of the sea surface temperature (SST) in the tropical region: the average SST in the latitude band from 20°S to 20°N was warmer “by about 0.3–0.4°C in the 1980s than in the 1970s,” and an even larger increase of SST was found in some individual regions of the tropical Pacific and Indian Ocean. Concurrently, the SST in the midlatitude North Pacific was decreasing. Disturbed by these SST anomalies, atmospheric circulations showed noticeable changes. In the Tropics, atmospheric convection became more active in the 1980s than in the 1970s. In the middle latitudes, “substantially lowering of the 500 hPa geopotential height and surface pressure (were observed) in the North Pacific,” and the

Pacific–North American anomaly pattern in northern winter strengthened after the late 1970s.

After these findings, additional analyses described an alternation of a dipolar SST anomaly in the tropical and central North Pacific Ocean (now known as the Pacific decadal oscillation). From the 1970s to the 1980s, this SST pattern reversed from the previous one and showed positive SST anomalies in the Tropics and negative anomalies in the central North Pacific. This anomaly pattern has persisted from the later 1970s through the 1990s (Zhang et al. 1997; Trenberth and Hoar 1997; Hu and Feng 2001a). Associated with the reversal of the SST pattern, Zhang et al. (1997) showed that “the time series of El Niño–Southern Oscillation (ENSO) indices . . . exhibit a break or regime shift from 1976 to 1977.” A simultaneous climate “regime shift” also was detected in the Northern Hemisphere (NH) midlatitudes, showing the diminishing of a once-strong ENSO teleconnection effect on the summer rainfall variation in the central United States (Hu and Feng 2001a,b), and a significant increase of the annual precipitation in the contiguous United States since the late 1970s (e.g., Karl et al. 1996).

These observed regime shifts suggest changes in the

* University of Nebraska Agricultural Research Division Contribution Number 14365.

Corresponding author address: Dr. Qi Hu, School of Natural Resource Sciences, 237 L. W. Chase Hall, University of Nebraska at Lincoln, Lincoln, NE 68583-0728.
E-mail: qhu2@unl.edu

NH atmospheric circulation in the late 1970s and early 1980s. However, these changes have not been examined except for being implicitly expressed by changes of the atmospheric mass field and by various climate indices and parameters. For example, both the analyses of Nitta and Yamada (1989) and Zhang et al. (1997) described changes of the SST and geopotential height patterns, and Nitta and Yamada further contrasted the average atmospheric geopotential height field between the two periods, 1967–76 and 1977–86. The recent work of Hu and Feng (2001a) depicted changes of the relationship of indices and parameters measuring circulations at regional scales in the North Pacific and North America. Thus, several questions remain regarding the NH atmospheric circulation change in the late 1970s, including (a) were there significant changes in the NH atmospheric circulation associated with the rise of the NH average surface temperature (Vautard et al. 1992) and the regime shift in the North Pacific Ocean in the late 1970s, (b) what were these changes, and (c) how could they be measured?

A way to measure the hemispheric and global atmospheric circulation change is by the atmospheric energetics. As delineated in Lorenz (1967), the energetics describe the atmospheric processes that convert the solar energy into the available potential energy and then the kinetic energy to maintain the circulation against both thermal and mechanical dissipations. Thus from examining the energetics we can identify changes of the processes maintaining the atmospheric circulation and hence changes of the circulation. For example, from changes of the available potential energy and kinetic energy and their exchange after the late 1970s we can uncover the roles of the SST change and the rising NH surface temperature in the atmospheric circulation change. In addition to illuminating new properties of atmospheric processes—for example, zonal and eddy energy exchanges—in the warmer climate, the atmospheric circulation change derived from the energetics can assist us to understand the recent changes of the frequency and intensity of the cyclones and anticyclones in the NH (e.g., Agee 1991; McCabe et al. 2001).

In this study, we examine the NH atmospheric energetics in the “traditional framework” of Lorenz (Lorenz 1955; Saltzman 1957). As discussed in Lorenz (1955) and illustrated in Plumb (1983), there are different ways to view the atmospheric energy cycle, particularly exchange/conversion between different forms of the energy. In the traditional framework, the Reynolds’s assumption is used to decompose the motion into mean flow and deviation from it, referred to as eddies. Consequently, the energy cycle consists of generation, exchange, and dissipation of potential and kinetic energies for both the mean flow and eddies. Plumb (1983) showed that this framework is inconvenient to show the energy cycle associated with some special wave motions. He suggested an alternative way to understand the energy cycle based on the Eliassen–Palm (EP) dy-

namics (Edmon et al. 1980) and the residual circulation concept. Although Plumb’s scheme highlighted some features in energy processes associated with those wave motions, his scheme’s application may be best for small-amplitude wave motions because the EP dynamics are relevant for such variations superimposed on pure zonal flows (Andrews 1987). For a more general problem such as the one dealt with in this study, the traditional framework is more relevant and it avoids limitations associated with assumptions in the EP dynamics.

In this traditional framework, we will calculate the NH atmospheric energetics using the National Centers for Environmental Prediction–National Center for Atmospheric Research (NCEP–NCAR) reanalysis data from 1948 to 2000 and address the previous questions by comparing and contrasting the energetics before and after the late 1970s, when a substantial increase of the surface air temperature and shifts of climate regimes occurred. Details of the data, particularly their quality and potential biases affecting changes in the energetics, and calculations of the energetics are described in the next section. In section 3, we present the major results of NH annual average and seasonal energy cycles and their changes in the late 1970s. Because the conversion mechanisms from the atmospheric available potential energy to kinetic energy is considerably different between the Tropics and the extratropics, we also examine energetics in three different latitudinal bands, the Tropics, the midlatitudes, and the high latitudes, and their contributions to changes of the hemispheric energetics. The energetics are further examined in wavenumber domain for different waves in the atmosphere representing planetary, synoptic, and storm-scale circulations. A summary of this study is presented in section 4 along with a discussion on manifestation of changes of the atmospheric energetics in intensity and frequency of storm and extreme weather in the mid- and high latitudes.

2. Data and methods

Monthly data of the variables—zonal, meridional, and vertical wind speed, air temperature, and geopotential height—from 1948 to 2000 are obtained from the NCEP–NCAR reanalysis dataset (Kalnay et al. 1996) and are used in this study. These are “type A variables” with the highest data quality rating in the reanalysis dataset (Kalnay et al. 1996). The horizontal resolution of the data is 2.5° latitude \times 2.5° longitude. In the vertical direction, these data are at the standard pressure levels: 1000, 850, 700, 600, 500, 400, 300, 250, 200, 150, 100, and 50 hPa.

There are several caveats in the reanalysis data. Three of which are discussed here because of their potential effects on this study’s results. First, because of fewer land-based observations in the Southern Hemisphere (SH), the reanalysis data for the SH showed larger root-mean-square errors from the true observations than the

data for the NH (Kistler et al. 2001). For this reason, we have limited our study to the NH. Second, weather observation systems, including surface and radiosonde sensors and observation schedule/frequency and methods, were upgraded and changed over the last 5 decades (especially in the *early* 1970s), and each of those changes had influenced the observation data, resulting in certain biases in the data to various degrees of magnitude. Most of the influences were evaluated and minimized to the best possible extent through quality control and assimilation schemes designed and used to develop the reanalysis dataset (Kalnay et al. 1996). As shown in Kistler et al. (2001), for the NH, because the zonal mean number of observations per 2.5° latitude–longitude box per month was adequate in the 1950s, the data quality of the type A variables in the reanalysis dataset has been “fairly uniform” from 1950s to the present, albeit the mean number of observations has increased since the 1950s (see Figs. 1 and 4 in Kistler et al. 2001). As further elaborated in Kistler et al., this consistent quality in the NH reanalysis data has resulted from two features of the reanalysis system: 1) “with a modern four-dimensional data assimilation system [in the reanalysis] even the early upper-air observing system can produce fairly skillful initial conditions in the NH,” and 2) the reanalysis system is skillful to produce week-long NH forecasts (see Figs. 5 and 6 in Kistler et al.), which were further used to develop, and hence warranted the quality of, the reanalysis data.

The consistent accuracy of individual type A variables in the reanalysis dataset also has been examined and discussed in several case studies. For example, Graham and Diaz (2001) show that the pressure data in the reanalysis dataset describe accurate spatial and temporal variations in sea level pressure over the North Pacific Ocean. One other study is on the NH storm track variation by Harnik and Chang (2003), examining the variance of the 300-hPa meridional wind (v'). Harnik and Chang contrasted v' from the reanalysis data and from available radiosonde data in several NH storm track entrance and exit regions from 1949 to 1999 (see Fig. 1b in Harnik and Chang 2003). Their results show a similar intensification of the storm tracks in both the North Atlantic and the North Pacific regions in recent decades from the two datasets although the intensification in the radiosonde data was weaker for the North Atlantic storm track and was not as significant as that from the reanalysis data in the North Pacific region. These differences have highlighted a spatial variation of the accuracy of v in the reanalysis data; the v' may be overestimated in the reanalysis data for some of those storm entrance and exit regions. Although this potential inaccuracy should always be kept in mind in evaluating calculations of the energetics in this study, the fact that the difference in v' is large only in the early 1970s (1970–73, instead of being in the late 1970s and early 1980s when noticeable changes developed in atmospheric circulations) and the equally valid notion that

“it is possible that an intensification of the (North) Pacific storm track did occur, but the sonde data is too sparse to say anything about it” (Harnik and Chang 2003) seem to support an adequate quality of the reanalysis’ meridional wind data.

The third concern arises from the use of satellite data since 1979. The use of the satellite observations in four-dimensional data assimilation increased the number of data sources for developing the reanalysis dataset. However, this improvement also brought with it a possibility that the data after 1979 could have contained artificial differences from the data before 1979. These differences and the seriousness of their effect on the data consistency were examined in Kistler et al. (2001). In fact, after showing the two features described in the second paragraph of this section, Kistler et al. examined those same features with and without use of the satellite data in the decades after 1979. Their results indicated similar skills of the reanalysis system in producing both initial conditions and forecasts from use or not use of the satellite data, thus demonstrating no persistent biases were produced in the data after 1979 from using the satellite data.

Using the reanalysis data, we calculate the annual and seasonal atmospheric energetics and energy cycle in the traditional framework derived using the primitive equations of motion on a sphere. Because many early studies have detailed the derivations of the energetics in such a setting (Lorenz 1955, 1967; Saltzman 1957; Oort 1964; Krueger et al. 1965; Kung and Soong 1969; Oort and Peixóto 1974), we only list in appendix A the energy terms and energy conversions in that framework for reference purposes. In our calculations, the atmospheric available potential energy, P , includes two parts: the mean available potential energy, P_M , and the eddy available potential energy, P_E , which is the sum of standing and transient eddy available potential energy; the kinetic energy, K , also consists of the mean kinetic energy, K_M , and the eddy kinetic energy, K_E , which has contributions from both the standing and transient eddies (Lorenz 1955). The total atmospheric energy is calculated by integration over the NH and in the vertical direction. The vertical integration is from 1000 to 50 hPa. At 50 hPa, the energy exchange with the higher stratosphere is neglected because such exchange is trivial to the tropospheric energy cycle (Kung and Tanaka 1983). In the meridional direction, the cross-equatorial energy fluxes are computed using the method described in Oort and Peixóto (1974).

To examine atmospheric energetics for motions of different scales from planetary, synoptic, to storm circulations, we also calculate the energetics in the wavenumber domain. An outline of the energetics in wavenumber forms is given in appendix B following the work of Saltzman (1957). In addition, we examine the energetics in three latitude bands, 0° – 30° N (Tropics), 30° – 60° N (midlatitude), and 60° – 90° N (high latitude), by applying the same methods used in the hemispheric cal-

culations. This analysis is necessary because changes in, for example, kinetic energy in NH could result primarily from variations in either the tropical or the extratropical regions, or both. The generation and conversion mechanisms from available potential energy to kinetic energy are, however, considerably different between the Tropics and the extratropics. In the Tropics, the mechanism is the direct circulation (Hadley cell) driven by convection and diabatic heating, whereas in the extratropics it is the baroclinic instability. Thus, knowing the latitudinal regions contributing to the energy cycle changes is essential for understanding mechanisms that may have caused the energetics change in recent decades. The separation of these latitudinal bands is based on variations in the zonally averaged meridional momentum flux from the equator to the North Pole (Fig. 1.10 in Palmen and Newton 1969) and associate features to different *zonal-mean* atmosphere circulation regimes in the NH (Holton 1979). In calculations of the energetics in the three latitude bands, we only consider energy generation and conversion within a band and neglect energy exchange across the latitude boundaries of the band.

3. Results and discussions

Using the monthly data from the reanalysis dataset we calculated the NH energetics and energy cycle in the troposphere and lower stratosphere. Before discussing the energy cycle, we show in Fig. 1 the variations of the NH summer (June, July, and August) mean kinetic energy (K_M), eddy kinetic energy (K_E), and total kinetic energy ($K = K_M + K_E$). A major feature in the variations is that the K_M (Fig. 1a) shows two different “regimes” before and after the late 1970s. Before the late 1970s, K_M was small and primarily below the average value of mean kinetic energy for the period 1948–2000. After 1980, K_M gradually rose and remained above the average. A Student’s t test showed that this change is significant at the 99% confidence level. Variations of the summer K_E in Fig. 1b also indicate a large change after the early 1980s. Before 1980, except for a period of high K_E centered in the mid-1970s, K_E was mostly below the average eddy kinetic energy for the period 1948–2000. Since 1980, K_E has increased substantially and has remained above the average. This change in K_E around 1980 also has been tested significant above the 95% confidence level. Combining the K_M and K_E , we show in Fig. 1c the variations of K . The total kinetic energy shows a similar change in the late 1970s.

Similar changes in K_M , K_E , and K in the late 1970s and early 1980s also have been found in the NH winter (December, January, and February; Fig. 5d). These results show significant rise of the NH kinetic energy in the late 1970s and indicate changes of the processes governing the NH atmospheric circulations when the warming of the average NH surface temperature and climate regime shift occurred. To quantify the changes

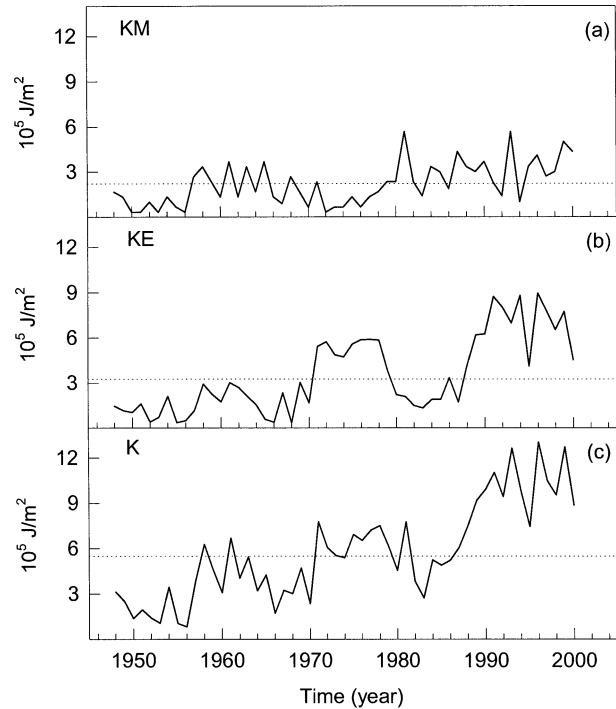


FIG. 1. Variations of the NH summer atmospheric (a) mean kinetic energy, (b) eddy kinetic energy, and (c) total kinetic energy. The dotted line shows the avg of 1948–2000.

of the atmospheric energy cycle in recent decades, we calculated the atmospheric available potential energy and kinetic energy and compared and contrasted various conversions between different energy pools before and after the late 1970s. These results are presented in the following sections.

a. Changes of the NH summer season atmospheric energetics

The NH summer season atmospheric energy cycle is shown in Fig. 2 for the two epochs, 1948–78 and 1979–2000. Comparisons of the two energy cycles show that the K_M has increased by 86%, and K_E increased by 70% from the former to the latter epoch. Quite different from the changes in the kinetic energy, however, a much smaller increase of merely 14% is shown in the eddy available potential energy, P_E , while the mean available potential energy, P_M , remains unchanged in the two epochs even though the potential energy generation, \overline{G} , has increased in the recent epoch. (Note that to avoid using poor quality types B and C variables of the reanalysis data in our calculations, the mean and eddy potential energy generation terms and dissipations of the mean and eddy kinetic energy were calculated as residues to balance the major mean and eddy energy terms, which were calculated using only type A variables.) The large increase of the kinetic energy and nearly unchanged available potential energy may be explained by an in-

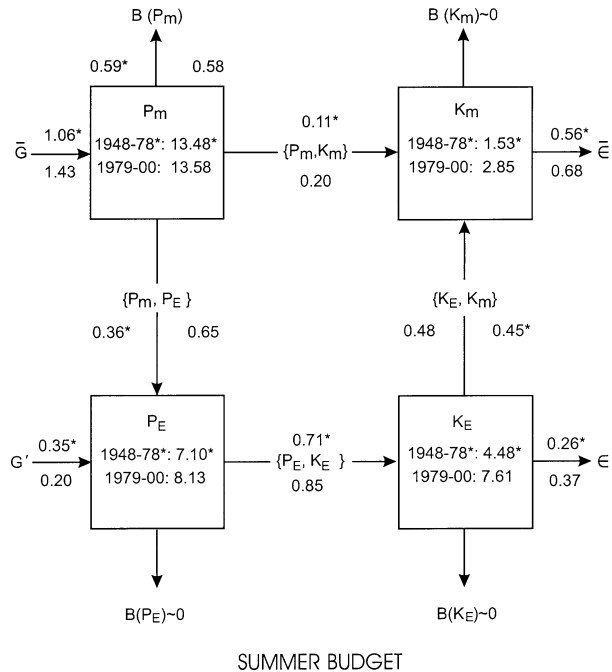


FIG. 2. Northern Hemisphere summer season energy cycle for the two epochs. The energy values and conversion rates for the epoch 1948–78 are shown with an asterisk. Conversion rates are written by the arrow lines. Other notations; \bar{G} and G' are generations of mean and eddy available potential energy, respectively, $\bar{\epsilon}$ and ϵ' are dissipations of mean and eddy kinetic energy, respectively, and B is the crossing equatorial exchange of energy. Units are W m^{-2} for energy conversion rate and 10^5 J m^{-2} for energy.

crease of the conversion rates from P_M to K_M , and from P_M to P_E , and then from P_E to K_E in the recent epoch. With the increased conversion rates, the increase of P_M generation could be quickly converted to the kinetic energy and result in the significant increases of both K_M and K_E . Compared to the net increase of the total energy generation ($0.05 \times 10^5 \text{ J m}^{-2}$), the nearly unchanged P_M and the large increase of the kinetic energy highlight a rising efficiency of the atmospheric thermal engine in the recent warmer climate.

The increased conversion rate from the available potential energy to the kinetic energy may be partially interpreted from changes in the NH summer season atmospheric temperature profile from 1948 to 2000. These changes are shown in Fig. 3 using temperature at three pressure levels, 50, 300, and 850 hPa. Figure 3 depicts a continuous increase of the temperature in the lower troposphere (Fig. 3c) along with an increase of the surface air temperature after the late 1970s. Temperatures in the upper troposphere (Fig. 3b) have remained nearly unchanged, however, while the temperature in the lower stratosphere has decreased considerably (Fig. 3a). These changes of the temperature profile in the recent epoch and the tendency to enrich the moisture content in the troposphere because of warming contribute to a decrease of the average atmospheric static stability. Indeed, weakening static stabilities in the recent warmer decades

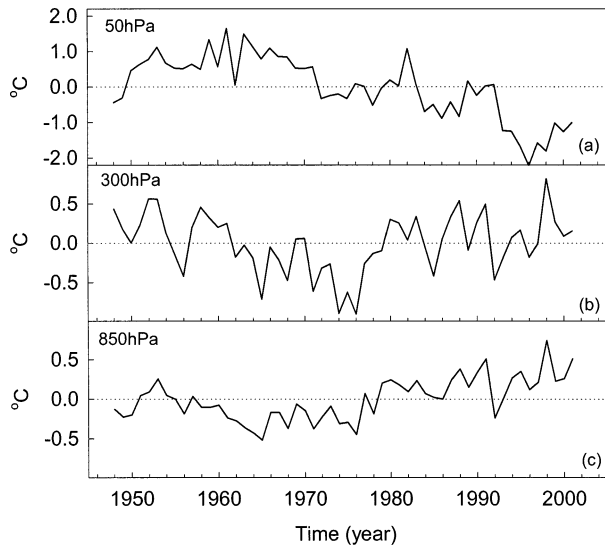


FIG. 3. Variations of the NH summer season avg temperatures at three pressure levels. The mean temperatures of the series have been removed.

after 1980 have been observed in several studies on regional climate variations (e.g., Trenberth 1999; Hu and Feng 2001a).

An atmosphere of weaker static stability with a warmer and moister surface layer encourages both dry and moist convection in the troposphere. Consequently, convection-induced subsidence motion, a vertical motion required by mass continuity to compensate the rising motion in convection, attempts to maintain a nearly steady temperature profile in the troposphere, around the dry or moist adiabatic lapse rate, as required by the thermodynamic property of the atmosphere.¹ By enhancing the overturning process in the atmosphere, moist convection converts available potential energy to the kinetic energy by moving the lighter warm and moist air up and denser cold and dry air down to lower the center of the tropospheric air mass. Some of the effects of static stability are shown by the role of the atmospheric stability in the formula for calculation of both the available potential energy and its conversion to the kinetic energy (appendix A), while the increase of convection in an atmosphere with such a thermal profile seems to be supported by observations of an increase in convective cloudiness in the NH midlatitudes in recent decades (e.g., Sun et al. 2001). These processes

¹ Combining the First and Second Law of Thermodynamics, we can arrive at $de = Tds - pdV - \delta Q'$, where e is internal energy, T the temperature of a heat source, s entropy, V volume, and $\delta Q'$ the heating. After some manipulations and integration over the tropospheric column, Z , we can get from the previous equation that $(c_p \gamma + g)Z = T_s S - Q$, where γ is the lapse rate, T_s the surface temperature, S the total entropy, and Q the irreversible heating of convection. Because the convective heating tends to balance the entropy change due to increase of T_s , the atmospheric lapse rate γ remains nearly a constant.

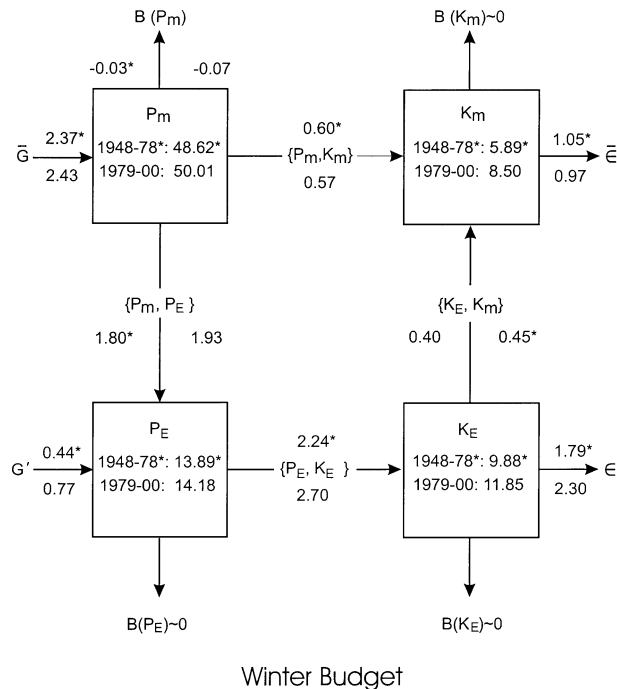


FIG. 4. Northern Hemisphere winter energy cycle for the two epochs. Notations are the same as in Fig. 2.

associated with the thermodynamic properties of the atmosphere maintain a nearly steady available potential energy by consuming its increased amount into the kinetic energy and atmospheric motion. As a result, the NH atmospheric available potential energy has changed a little corresponding to the increase of the surface temperature, and the effect of warming in recent decades has manifested primarily in the increase of the atmospheric kinetic energy.

b. Changes of the NH winter season atmospheric energetics

Similar to the changes in the summer season energetics, the NH winter season energetics also shows an increase of the kinetic energy and nearly unchanged available potential energy in the recent epoch (Fig. 4). Notice that all the energy forms, particularly the mean available potential energy, have a much larger amount in winter than in summer. Among the increase of the winter kinetic energy in the recent epoch, K_M has been up by 44%, which is statistically significant at the 95% confidence level, and K_E has been up by 20%, marginally significant at the 90% confidence level. Although both P_M and P_E show little change in the recent epoch, they do not, however, indicate similar winter season energetic processes in the two epochs. This is suggested by the larger increase in the generation of total available potential energy ($0.39 \times 10^5 \text{ J m}^{-2}$), primarily from G' , a result showing more potential energy was generated and converted to the kinetic energy in winters of the

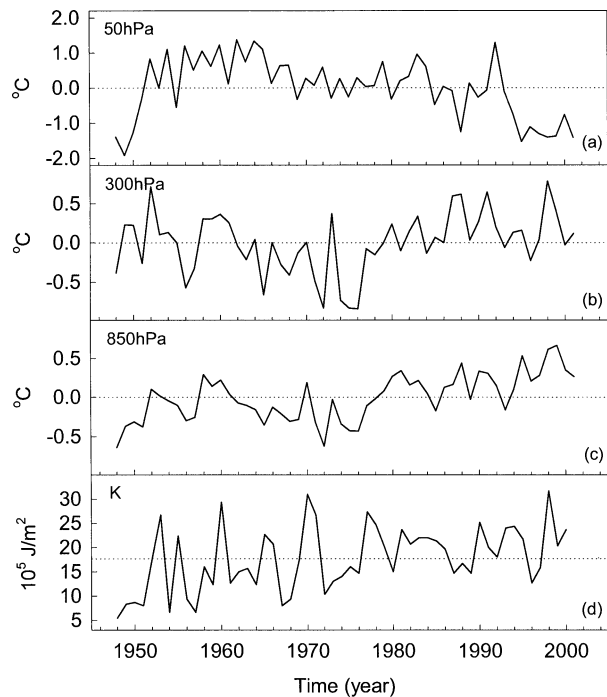


FIG. 5. (a)–(c) Variations of the NH winter avg temperatures at three pressure levels. (d) Variation of the NH winter total kinetic energy with the dotted line showing its avg for the period 1948–2000.

recent epoch. After examining the conversion and dissipation rates, we found a large increase of the conversion primarily from P_E to K_E and an increased dissipation of K_E .

The large conversion from the available potential energy to the kinetic energy in the NH winter also prompted us to examine the NH winter season temperature variations in a way similar to what we did for the northern summer. The temperature variations in the three pressure levels, 50, 300, and 850 hPa, are shown in Figs. 5a–c. First, the variations show similarly strong contrasts between the two epochs. For example, the temperature at 850 hPa was relatively steady in the early epoch and has become persistently warmer than the period average in the recent epoch (Fig. 5c). A significant decrease was observed in 50-hPa temperature (Fig. 5a). These changes of the atmospheric temperatures are similar to that in the NH summer and suggest changes in atmospheric processes that have effectively converted the increased available potential energy to the kinetic energy. Increase of the NH winter season mean kinetic energy in the recent epoch is clearly shown in Fig. 5d.

c. Changes of the NH atmospheric energetics in spring and autumn

In the transition seasons of spring (March, April, and May) and autumn (September, October, and November), the change of both the available potential energy and

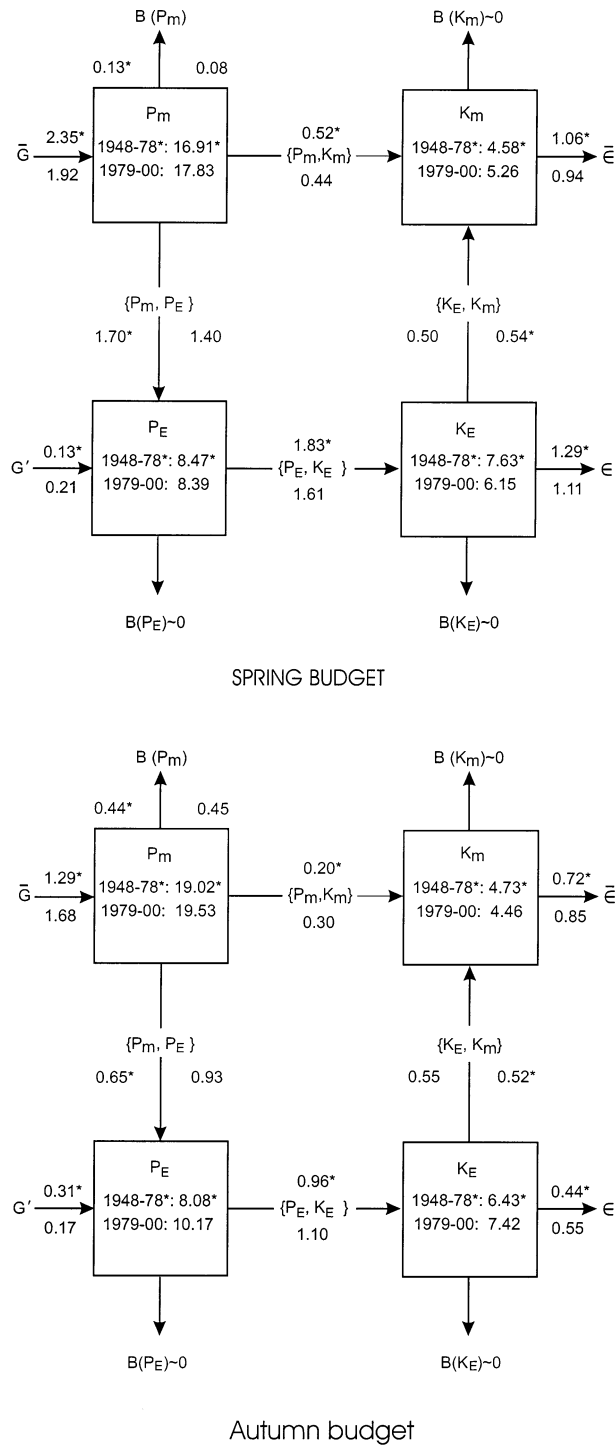


FIG. 6. Northern Hemisphere (top) spring and (bottom) autumn energy cycle for the two epochs. Notations are the same as in Fig. 2.

the kinetic energy between the two epochs are small and insignificant (Fig. 6). In fact, the spring season energy cycle is weaker in the recent epoch. The generation of the potential energy and conversion from the avail-

able potential energy to the kinetic energy are both smaller in the recent epoch than in the previous one. In autumn, the K_M has decreased in the recent epoch although a slight increase of other forms of energy is observed. The nearly unchanged energetics in the transition seasons indicate that the atmospheric circulation change in the recent epoch has occurred primarily in the NH summer and winter.

d. Changes of the atmospheric energetics in different latitudes

The previous sections described variations of the energetics averaged over the NH. Changes in these hemispheric averages can be attributed to changes in different latitudes and from very different mechanisms. For example, in the tropical region, change in conversion from the available potential energy to the kinetic energy would result from anomalies in convective overturning and associated direct circulation, whereas in the mid-latitudes the conversion would result from anomalies in overturning associated with release of baroclinic instability and vertical motions in cyclonic waves. Because of these different mechanisms, it is important to separately examine variations of the energetics at different latitudes and their contributions to change of the NH energy cycle. We have examined the energetics in three different latitudinal bands, Tropics (0° – 30° N), midlatitudes (30° – 60° N), and high latitudes (60° – 90° N), and their relationship with the average NH energetics. The results are shown in Fig. 7.

In the tropical region, both the available potential energy and the kinetic energy show small changes after the late 1970s, most of them showing a decrease. In contrast to the substantial changes of the kinetic energy in the midlatitudes, these small changes in the tropical region indicate that the significant increase of the NH kinetic energy in recent decades has resulted primarily from increases of the atmospheric energy in the mid- and high latitudes.

From examining the energetics for the mid- and high latitudes in Fig. 7, we also find that changes of both the available potential energy and the kinetic energy have smaller magnitudes in the high-latitude region than in the midlatitude region. In the midlatitudes, the most significant change is in the kinetic energy; both the mean and eddy kinetic energies show large increases in the recent epoch. The increases of both K_M and K_E are shown in the NH winter and summer seasons. These increases suggest enhanced winter and summer season weather disturbances in the midlatitudes with the warming in the late 1970s.

It is intriguing that the substantial increase of mid-latitude K_M and K_E in the recent epoch occurred simultaneously with a nearly unchanged available potential energy and a slight decrease of the total kinetic energy in the tropical region. A plausible explanation of this little change in energetics of the tropical region

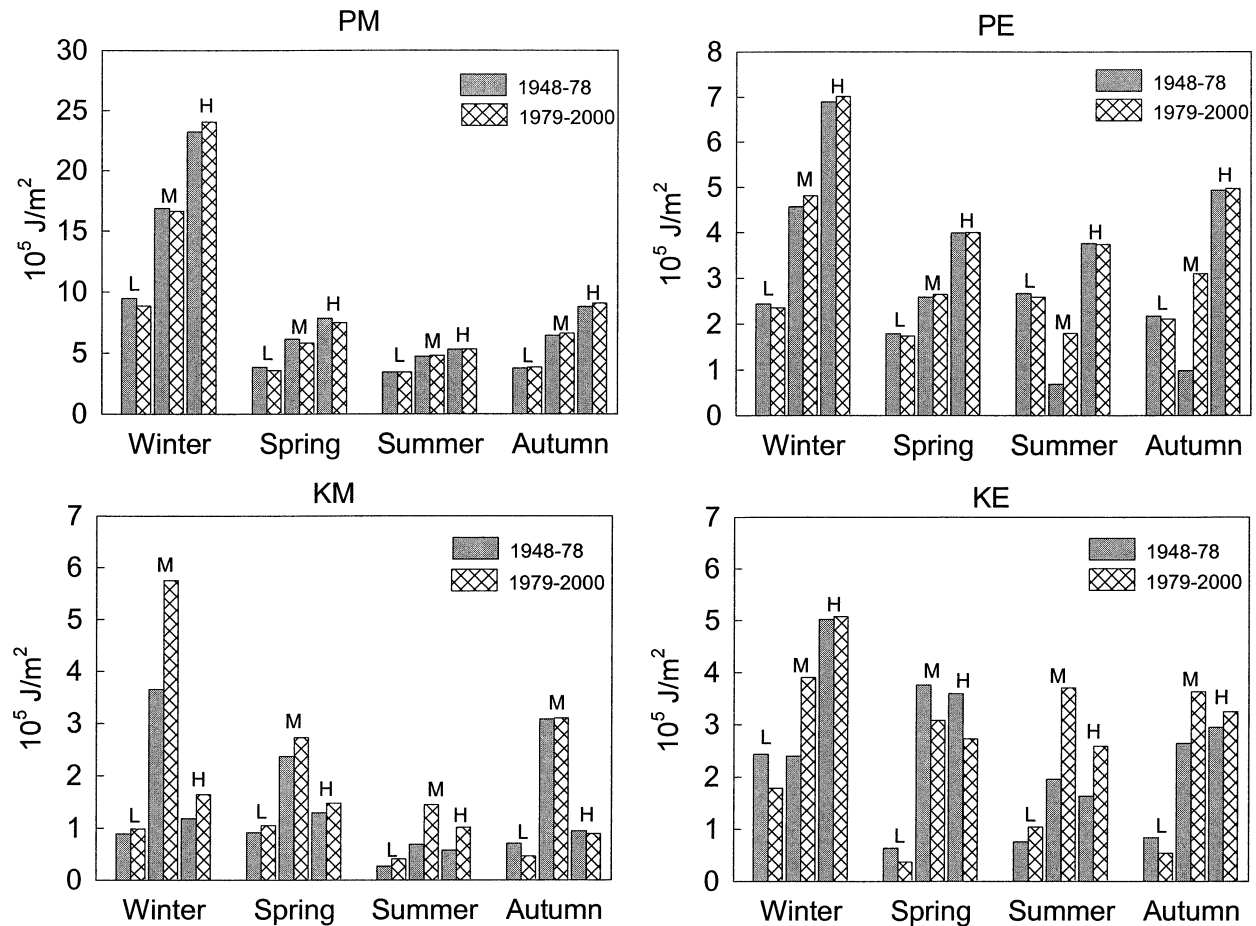


FIG. 7. Comparisons of the NH mean (PM) and eddy (PE) available potential energy and mean (KM) and eddy (KE) kinetic energy in different latitude bands (L: Tropics; M: midlatitude; H: high latitude) and for different seasons between the two epochs.

could be a negative evaporation feedback to increasing SST and longwave radiation similar to that elaborated in Hartmann (1994). This feedback limits the increase of the SST and its potential effect on changes of the atmospheric energetics in the tropical region. Because a similar feedback is lacking in the midlatitudes, the increase in midlatitude surface temperature could have increased the meridional temperature gradient to the polar region so that the baroclinicity and the rate of conversion from the available potential energy to the kinetic energy increased in the midlatitudes. Supporting evidence of the increase in midlatitude baroclinicity in recent decades has been presented in Paciorek et al. (2002). The observed increased frequency of the synoptic disturbances in the midlatitudes also could have been assisted by more cyclones moving from lower latitudes to the midlatitudes. These cyclones further develop in the midlatitudes oceanic regions with warmer SST (Walsh and Katzfey 2000). By carrying the kinetic energy to the higher latitudes, these cyclones could have contributed to the observed decrease in eddy kinetic energy in the tropical region (Fig. 7), creating an apparent shift of some atmospheric kinetic energy from

the tropical to the midlatitudes region in the warmer climate.

e. Changes of the NH atmospheric energetics in wavenumber domain

So far, we have shown the changes of the available potential energy and the kinetic energy in the NH and in different latitude regions. These are integrated results of variations over various wave components constituting weather and climate of wide spatial and temporal scales, from planetary circulation to regional storms. It is necessary to understand how these variations have comprised changes in energetics of different wave components representing these different weather regimes. Energy changes of the individual wave components can assist us to find how the circulation systems of planetary to storm scales have changed following the change of the energetics.

The methods applied in calculations of P_M , P_E , K_M , and K_E for different wave components are discussed in appendix B after the work of Saltzman (1957). Results of the calculations show that the available potential en-

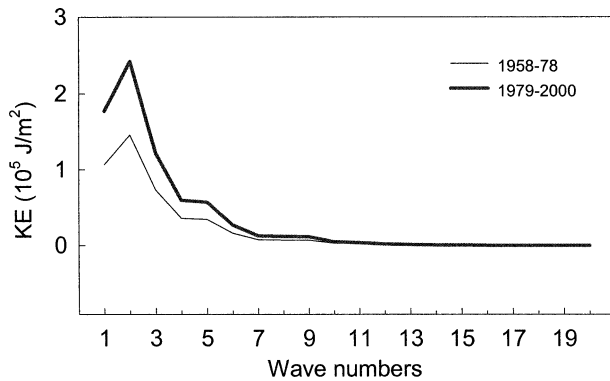


FIG. 8. Comparisons of the NH eddy kinetic energy of different wave components between the two epochs.

ergy changed little in individual waves before and after the late 1970s, but statistically significant changes occurred in both summer and winter season K_E and K_M for most waves of low wavenumbers (large spatial scales). Because of their similar changes in winter and summer season kinetic energy, we only show summer season K_E change for wavenumbers 1–20 in Fig. 8. Before discussing the changes in K_E , we notice that among these wave components wavenumbers 2 and 1, representing the planetary circulation, have the largest K_E . Waves of wavenumbers 3–5, representing synoptic-scale disturbances, also have substantial K_E in the summer season. Much smaller amount of K_E resides in waves of higher wavenumbers. This general distribution of kinetic energy in the wavenumber domain is consistent with the result of Kung and Tanaka (1983). With respect to changes of K_E after the late 1970s, a comparison of the results in Fig. 8 indicates an increase of K_E in the recent epoch. Although this increase is apparently large for waves of wavenumbers 1–7, the changes relative to the K_E of each wavenumber, or the percentage increase in K_E of individual waves, is comparable among the waves of wavenumbers 8–20. This result suggests a recent increase of synoptic disturbances and regional severe storms, consistent with the observations in Paciorek et al. (2002), who showed rising Eady Growth Rate and temperature variance in the region 20° – 70°N , and in Agee (1991) who showed increasing frequency and intensity of cyclones/anticyclones in most of the NH in recent decades. A Student's t test has confirmed that the increase of the summer K_E in the waves of wavenumbers 1–20 are significant at the 95% confidence level.

Similar distribution and increase also have been found in winter K_E and in the mean kinetic energy across the same wavenumber waves. Although K_M is 2 to 3 times larger in the NH winter than summer, the percentage of increase of K_M in recent decades is comparable between the two seasons, and the change is statistically significant.

4. Summary and concluding remarks

In this study, we used the NCEP–NCAR reanalysis data and examined the NH atmospheric energetics in the traditional framework of Lorenz. The purpose is to use the energetics as a measure to evaluate changes of the NH atmospheric circulation associated with the rising surface temperature and climate “regime shift” in the late 1970s and the early 1980s. It is important to bear in mind that some caveats in the reanalysis dataset, resulting from changes of observational networks over the history and integrations of modern data systems in recent decades, could have influenced the outcome of our calculations. Nonetheless, our evaluations of the existing work that have scrutinized the dataset and its variables from different aspects have assured us adequate quality and accuracy of the data for our purpose. Based on our evaluations, the identified signs in the changes of the atmospheric energy cycle should hold in the results albeit minor differences in the magnitude of the changes may be possible.

Among the major results of this study, the comparisons of the atmospheric energetics between the two epochs of 1948–78 and 1979–2000 have uncovered significant increases of the NH summer and winter season kinetic energy, both K_M and K_E , in the recent epoch. The increase has resulted from increased conversion rates from the mean to the eddy available potential energy and then from the eddy available potential energy to the eddy and mean kinetic energy. Direct conversion from the mean available potential energy to the mean kinetic energy also has increased. Owing to the increased conversion rates, the atmospheric available potential energy has remained nearly steady in the two epochs, even though generation of the available potential energy has increased in the recent decades of warmer climate. Associated with the increased conversion rates is the enhanced vertical overturning of the air mass and meridional circulation that lower the center of the air mass and, in doing so, convert the increased available potential energy to the increase of both the mean and eddy kinetic energy of the zonal flow. Although the changes of the kinetic energy in the transition seasons (spring and autumn) are small between the epochs, the significant kinetic energy increase in the NH summer and winter describes considerable changes of the NH general circulation occurred concurrently with the increase of the NH average surface temperature.

In addition, changes of the atmospheric kinetic energy in different latitude bands indicate that the increase of the NH kinetic energy has resulted primarily from the increase in the midlatitudes, because the kinetic energy in the tropical region has decreased slightly in the recent epoch. These opposite changes of the kinetic energy between the Tropics and midlatitudes is speculated to result from the presence of a negative evaporation feedback to increasing SST and longwave radiation in the tropical region and a lack of it in the mid- and high

latitudes (Hartmann 1994). The changes of the midlatitude SST pattern also could have encouraged cyclones to travel over warm SST regions from low to midlatitudes and to further develop in the midlatitudes (Walsh and Katafey 2000). By carrying portions of kinetic energy from low to midlatitudes, these long-lived cyclones could have not only contributed to the increase of the kinetic energy in the midlatitudes but also created an apparent shift of the kinetic energy from low to midlatitudes in the warmer climate. In the mid- and high latitudes, the increase of the conversion from the available potential energy to the kinetic energy in NH summer is consistent with the observed intensification of meridional temperature gradient and baroclinicity in mid- and high latitudes in recent decades (Paciorek et al. 2002).

Results of this study further show that the increase of the kinetic energy in NH summer and winter occurred in a wide range of wave components and scales of disturbances, from planetary (wavenumbers 1–2) to synoptic (wavenumbers 3–5) and to regional (wavenumbers 5 and higher). The increase is found comparable across these wave components, indicating similar percentage of energy increase in most atmospheric circulation systems. Because the tropical region has shown only small changes or a decrease in kinetic energy, the kinetic energy increase in those circulation systems have resulted from changes in mid- and high-latitude regions.

The changes of the atmospheric energetics in the mid- and high latitudes in the recent decades of warming climate may help explain some observed circulation changes. For example, several studies cited earlier reported changes of the frequency and intensity of the NH surface and midtroposphere cyclones and anticyclones. Agee (1991) examined three datasets covering different time periods from 1900 to 1985 and found increased (decreased) frequency of the NH cyclone and anticyclone in warmer (cooler) period, whereas Serreze et al. (1997) and McCabe et al. (2001) examined NH winter cyclone cases in 1966–93 and showed that the number of winter cyclones have decreased in midlatitudes and increased in high latitudes in the recent warmer climate after the late 1970s. Agee's results seem consistent with the average increase of both the mid- and high-latitude available potential energy and kinetic energy in recent decades. The especially large changes of the summer season energies (Fig. 7) and the increase of baroclinicity and the Eady Growth Rate in the NH (also see Paciorek et al. 2002) in recent warmer climate would indicate more disturbances in the NH mid- and high latitudes. When winter season is considered alone, the change of the energetics shows decreased (increased) mean available potential energy in the mid- (high) latitudes, suggesting stronger zonal flows with fewer cyclones.

The increase of the mean kinetic energy in both winter and summer seasons indicates enhancing zonal flow and a tendency for the zonal flow to work as a "dam" and impede the north–south exchange of eddy air masses.

This effect from increased mean kinetic energy seems counteracting to that of the increased eddy kinetic energy which represents increasing north–south exchange by eddies. A plausible explanation of this dilemma is that the eddy exchange would have behaved in a pulsating fashion with intensity high enough to meet the observed increase of the eddy kinetic energy when averaged over the decades. This new fashion of eddy energy exchange would correspond to more extreme and high-intensity weather events in the mid- and high latitudes, a possible explanation of the increase of intense cyclones and anticyclones in recent decades (e.g., McCabe et al. 2001; Pariorek et al. 2002). This interaction of mean and eddy kinetic energy and consequences to the extreme weather needs to be further examined in order to understand extreme weather behavior in a warmer climate.

Acknowledgments. We thank Dr. Ernest C. Kung for his assistance and discussion during our computation of the energetics. Thanks also go to three anonymous reviewers and the editor, Dr. S. Schubert, for their comments that led to improvements of this manuscript. This work was supported by NOAA under Grant 1445-CA09095-0069 to the University of Nebraska at Lincoln and by USDA Cooperative Research Project NEB-40-008.

APPENDIX A

Definitions of Atmospheric Energy and Energy Conversion Terms

The atmospheric available potential energy includes mean available potential energy, P_M , and eddy available potential energy, P_E . The latter is the sum of standing and transient eddy available potential energy. The kinetic energy consists of the mean kinetic energy, K_M , and the eddy kinetic energy, K_E . Similarly, K_E has two contributions from standing eddies and transient eddies (Lorenz 1955). These energy terms are expressed in forms of

$$P_M = \frac{c_p}{2} \int \gamma [\langle T \rangle]^{n-2} dm, \quad (\text{A1})$$

$$P_E = P_{TE} + P_{SE} = \frac{c_p}{2} \int \gamma [\langle T'^2 \rangle + \langle T \rangle^{*2}] dm, \quad (\text{A2})$$

$$K_M = \frac{1}{2} \int \{[\langle u \rangle]^2 + [\langle v \rangle]^2\} dm, \quad (\text{A3})$$

$$K_E = K_{TE} + K_{SE} = \frac{1}{2} \int [\langle u'^2 \rangle + \langle v'^2 \rangle] dm + \frac{1}{2} \int [\langle u \rangle^{*2} + \langle v \rangle^{*2}] dm, \quad (\text{A4})$$

where $\int [f] dm = \int_z \int_y \int_x f \rho dx dy dz$, and $\rho dx dy dz$ is the mass element of the atmosphere, and $\gamma =$

$-\{(\theta/T)[(R/c_p)P]\}$ is the stability factor defined in Oort (1964).

The energy conversions between different forms of energy are

$$C(P_M, K_M) = - \int [\langle v \rangle] g \frac{\partial[\langle z \rangle]}{a \partial \phi} dm, \tag{A5}$$

$$C(P_M, P_E) = -c_p \int \gamma[\langle v'T' \rangle + \langle v \rangle^* \langle T \rangle^*] \frac{\partial[\langle T \rangle]}{a \partial \phi} dm - c_p \int p^{-\kappa} [\langle w'T' \rangle + \langle w \rangle^* \langle T \rangle^*] \frac{\partial(\gamma p^\kappa [\langle T \rangle]')}{\partial p} dm, \tag{A6}$$

$$C(P_E, K_E) = - \int g \left[\left\langle \frac{u' \partial z'}{a \cos \phi \partial \lambda} \right\rangle + \left\langle \frac{v' \partial z'}{a \partial \phi} \right\rangle \right] dm - \int g \left[\frac{\langle u \rangle^* \partial \langle z \rangle^*}{a \cos \phi \partial \lambda} + \frac{\langle v \rangle^* \partial \langle z \rangle^*}{a \partial \phi} \right] dm, \tag{A7}$$

$$\begin{aligned} C(K_E, K_M) = & \int [\langle u'v' \rangle + \langle u \rangle^* \langle v \rangle^*] \cos \phi \left\{ \frac{\partial[\langle u \rangle / \cos \phi]}{a \partial \phi} \right\} dm + \int [\langle v'^2 \rangle + \langle v \rangle^{*2}] \frac{\partial[\langle v \rangle]}{a \partial \phi} dm \\ & + \int [\langle w'u' \rangle + \langle w \rangle^* \langle u \rangle^*] \frac{\partial[\langle u \rangle]}{\partial p} dm + \int [\langle w'v' \rangle + \langle w \rangle^* \langle v \rangle^*] \frac{\partial[\langle v \rangle]}{\partial p} dm \\ & - \int [\langle v \rangle][\langle u'^2 \rangle + \langle u \rangle^{*2}] \frac{[\tan \phi]}{a} dm, \end{aligned} \tag{A8}$$

where $C(A, B)$ represents conversion rate from energy A to B , and (A5) is an alternative expression for conversion of mean potential energy to mean kinetic energy. In the preceding, u and v are zonal and meridional wind speed, respectively, w is the vertical wind speed, T is the air temperature, a is the average radius of the earth, c_p is the specific heat of air at constant pressure, λ longitude, ϕ latitude, p pressure, g gravitational acceleration, z geopotential height, $\kappa = R/c_p$, and R is the gas constant for dry air. The time and zonal averages of a variable x are expressed by, $\langle x \rangle$, and $[x]$, respectively, and the departure of x from its zonal average is denoted by x^* , its departure from meridional average is x'' , and departure from its time average is x' .

APPENDIX B

Atmospheric Energetics in Wavenumber Domain

Because the kinetic energy is proportional to the product (square) of velocity and the potential energy is proportional to product (square) of temperature, we first discuss the Fourier integral of the product of two functions. Using Fourier integral in the zonal direction for functions $f(\varphi, \lambda)$ and $g(\varphi, \lambda)$, the Fourier transform of the product of f and g is (Saltzman 1957)

$$\begin{aligned} & \frac{1}{2\pi} \int_0^{2\pi} [f(\lambda)g(\lambda)]e^{-in\lambda} d\lambda \\ & = \frac{1}{2\pi} \int_0^{2\pi} f(\lambda) \left[\sum_{m=-\infty}^{\infty} G(m)e^{im\lambda} \right] e^{-in\lambda} d\lambda, \end{aligned}$$

where m and n are the zonal wavenumbers for functions f and g , respectively, $G(m)$ is the transfer coefficient of $g(\lambda)$, and φ is removed at a constant latitude. The preceding can be further written as

$$\begin{aligned} & \frac{1}{2\pi} \int_0^{2\pi} [f(\lambda)g(\lambda)]e^{-in\lambda} d\lambda \\ & = \sum_{m=-\infty}^{\infty} G(m) \frac{1}{2\pi} \int_0^{2\pi} f(\lambda)e^{-i(n-m)\lambda} d\lambda \\ & = \sum_{m=-\infty}^{\infty} G(m)F(n-m), \end{aligned}$$

where $F(n)$ is the transfer coefficient of f . Setting $g = f$, the preceding becomes

$$\frac{1}{2\pi} \int_0^{2\pi} f^2(\lambda)e^{-in\lambda} d\lambda = \sum_{m=-\infty}^{\infty} F(m)F(n-m),$$

and further setting $n = 0$, we get

$$\frac{1}{2\pi} \int_0^{2\pi} f^2(\lambda) d\lambda = \sum_{m=-\infty}^{\infty} |F(m)|^2, \tag{B1}$$

where $|F(m)|^2$ is the mode of coefficient F .

Applying (B1), we get mean and eddy kinetic energy in the wavenumber domain

$$K_M(n) = \frac{1}{2} \int [(\langle U(n) \rangle)^2 + (\langle V(n) \rangle)^2] dm, \text{ and } \tag{B2}$$

$$\begin{aligned}
 K_E(n) &= \frac{1}{2} \int [\langle U(n) \rangle'^2 + \langle V(n) \rangle'^2] dm \\
 &+ \int [\langle U(n) \rangle^{*2} + \langle V(n) \rangle^{*2}] dm \quad (\text{B3}) \\
 &= K_{TE}(n) + K_{SE}(n),
 \end{aligned}$$

respectively, where the integrations are over mass and n is the wavenumber and $n = 1, 2, \dots, \infty$. Applying the same procedure, we can get the potential energy in wavenumber domain

$$p_E = \sum_{n=1}^{\infty} R(n), \quad (\text{B4})$$

where $R(n) = (c_p/g)|B(n)|^2$, and $B(n)$ is the transfer coefficient of temperature at wavenumber n , $B(n) = 1/2\pi \int_0^{2\pi} T(n, \varphi, p, t)e^{in\lambda} d\lambda$. The conversion terms of energy in (A5)–(A8) in wavenumber domain are obtained by applying the preceding procedure to each of the terms.

REFERENCES

- Agee, E. M., 1991: Trends in cyclone and anticyclone frequency and comparison with periods of warming and cooling over the Northern Hemisphere. *J. Climate*, **4**, 263–267.
- Andrews, D. G., 1987: On the interpretation of the Eliassen–Palm flux divergence. *Quart. J. Roy. Meteor. Soc.*, **113**, 323–338.
- Edmon, H. J., Jr., B. J. Hoskins, and M. E. McIntyre, 1980: Eliassen–Palm cross sections for the troposphere. *J. Atmos. Sci.*, **37**, 2600–2616.
- Graham, N. E., and H. F. Diaz, 2001: Evidence for intensification of North Pacific winter cyclones since 1948. *Bull. Amer. Meteor. Soc.*, **82**, 1869–1893.
- Harnik, N., and E. K. M. Chang, 2003: Storm track variations as seen in radiosonde observations and reanalysis data. *J. Climate*, **16**, 480–495.
- Hartmann, D. L., 1994: Climate sensitivity and feedback mechanisms. *Global Physical Climatology*, Academic Press, 229–253.
- Holton, J. R., 1979: The general circulation. *An Introduction to Dynamic Meteorology*, Academic Press, 247–294.
- Hu, Q., and S. Feng, 2001a: Variations of teleconnection of ENSO and interannual summer rainfall variation in the central United States. *J. Climate*, **14**, 2469–2480.
- , and —, 2001b: Climatic role of the southerly flow from the Gulf of Mexico in interannual variations in summer rainfall in the central United States. *J. Climate*, **14**, 3156–3170.
- Kalnay, E., and Coauthors, 1996: The NCEP/NCAR 40-Year Reanalysis Project. *Bull. Amer. Meteor. Soc.*, **77**, 437–471.
- Karl, T. R., R. W. Knight, D. R. Easterling, and R. G. Quayle, 1996: Indices of climate change for the United States. *Bull. Amer. Meteor. Soc.*, **77**, 279–292.
- Kistler, R., and Coauthors, 2001: The NCEP–NCAR 50-year reanalysis: Monthly means CD-ROM and documentation. *Bull. Amer. Meteor. Soc.*, **82**, 247–267.
- Krueger, A. F., J. S. Winston, and D. A. Haines, 1965: Computation of atmospheric energy and its transformation for the Northern Hemisphere for a recent five-year period. *Mon. Wea. Rev.*, **93**, 227–238.
- Kung, E. C., and S. Soong, 1969: Seasonal variation of kinetic energy in the atmosphere. *Quart. J. Roy. Meteor. Soc.*, **95**, 501–512.
- , and H. Tanaka, 1983: Energetics analysis of the global circulation during the special observation period of FGGE. *J. Atmos. Sci.*, **40**, 2575–2592.
- Lorenz, E. N., 1955: Available potential energy and the maintenance of the general circulation. *Tellus*, **7**, 157–167.
- , 1967: *The Nature and Theory of the General Circulation of the Atmosphere*. World Meteorological Organization, 161 pp.
- McCabe, G. J., M. P. Clark, and M. C. Serreze, 2001: Trends in Northern Hemisphere surface cyclone frequency and intensity. *J. Climate*, **14**, 2763–2768.
- Nitta, T., and S. Yamada, 1989: Recent warming of tropical sea surface temperature and its relationship to the Northern Hemisphere circulation. *J. Meteor. Soc. Japan*, **67**, 375–383.
- Oort, A. H., 1964: On estimates of the atmospheric energy cycle. *Mon. Wea. Rev.*, **92**, 483–493.
- , and J. P. Peixoto, 1974: The annual cycle of the energetics of the atmosphere on a planetary scale. *J. Geophys. Res.*, **79**, 2705–2719.
- Paciorek, C. J., J. S. Risbey, V. Ventura, and R. D. Rosen, 2002: Multiple indices of Northern Hemisphere cyclone activity, winter 1949–99. *J. Climate*, **15**, 1573–1590.
- Palmen, E., and C. W. Newton, 1969: The mean structure of the atmosphere, and the maintenance of the general circulation in the Northern Hemisphere. *Atmospheric Circulation Systems: Their Structure and Physical Interpretation*, Academic Press, 1–25.
- Plumb, R. A., 1983: A new look at the energy cycle. *J. Atmos. Sci.*, **40**, 1669–1688.
- Saltzman, B., 1957: Equations governing the energetics of the larger scales of atmospheric turbulence in the domain of wave number. *J. Meteor.*, **14**, 513–523.
- Sereze, M. C., F. Carse, R. G. Barry, and J. C. Rogers, 1997: Icelandic low cyclone activity: Climatological features, linkages with the NAO and relationships with recent changes in the Northern Hemisphere circulation. *J. Climate*, **10**, 453–464.
- Sun, B., P. Y. Groisman, and I. I. Mokhov, 2001: Recent changes in cloud-type frequency and inferred increases in convection over the United States and the former USSR. *J. Climate*, **14**, 1864–1880.
- Trenberth, K. E., 1999: Conceptual framework for changes of extremes of the hydrological cycle with climate change. *Climatic Change*, **42**, 327–339.
- , and T. J. Hoar, 1997: El Niño and climate change. *Geophys. Res. Lett.*, **24**, 3057–3060.
- Vautard, R., P. Yiou, and M. Ghil, 1992: Singular-spectrum analysis: A toolkit for short, noisy chaotic signal. *Physica D*, **58**, 95–126.
- Walsh, K. J., and J. Katakafey, 2000: The impact of climate change on the poleward movement of tropical cyclone-like vortices in a regional climate model. *J. Climate*, **13**, 1116–1132.
- Zhang, Y., J. M. Wallace, and D. S. Battisti, 1997: ENSO-like interdecadal variability: 1900–93. *J. Climate*, **10**, 1004–1020.